The Effects of Hydrogen−Bonding Environment on the Polarization and Electronic Properties of Water Molecules

ARTICLE *in* THE JOURNAL OF PHYSICAL CHEMISTRY A · APRIL 2007

Impact Factor: 2.69 · DOI: 10.1021/jp067922u · Source: PubMed

2 AUTHORS:

Michael Devereux
University of Basel
23 PUBLICATIONS **294** CITATIONS

SEE PROFILE

Paul L A Popelier
The University of Manchester
190 PUBLICATIONS **7,111** CITATIONS

SEE PROFILE

The Effects of Hydrogen-Bonding Environment on the Polarization and Electronic Properties of Water Molecules

M. Devereux and P. L. A. Popelier*

Manchester Interdisciplinary Biocentre, University of Manchester, 131 Princess Street, Manchester M1 7DN, Great Britain

Received: November 29, 2006

Adequate representation of the interactions that take place between water molecules has long been a goal of force field design. A full understanding of how the molecular charge distribution of water is altered by adjacent water molecules and by the hydrogen-bonding environment is a vital step toward achieving this task. For this purpose we generated ab initio electron densities of pure water clusters and hydrated serine and tyrosine. Quantum chemical topology enabled the study of a well-defined water molecule inside these clusters, by means of its volume, energy, and multipole moments. Intra- and intermolecular charge transfer was monitored and related to the polarization of water in hydrogen-bonded networks. Our analysis affords a way to define different types of water molecules in clusters.

1. Introduction

Quantifying to what extent molecules are affected by their local environment in gas-phase clusters or in condensed matter is important. For example, it has long been known that polarization and cooperative effects are needed when modeling the bulk properties of liquid water.[1,2] Much effort has been invested in the accurate determination of cluster geometries and in trying to determine the physical properties of water molecules within these clusters. Water is central to the design of many force fields, but if we wish to accurately describe the interactions between individual water molecules or with the molecules they hydrate, we must account for polarization of their electron density.

Exploring the properties of molecules within clusters inevitably calls for a decision on how to partition a given system into its constituent molecules. Although increasingly sophisticated experiments and accurate quantum chemical calculations provide converging information[3−5] on molecular clusters and liquids, this convergence does not address the issue of partitioning. This is the reason why, for example, the dipole moment of a single water molecule in pure liquid water remains a matter of debate.[6] Values can vary as much as 2.3 to 3.1 D,[7] while experimental[8] and ab initio calculations[6,9] closely agree on 1.855 D for a single water's dipole moment in the gas phase. The ability to identify and characterize individual atoms in water clusters allows us to see changes in the charge density taking place and to use this information to reveal how the charge is redistributed throughout the molecule.

Demarcation of individual molecules that are part of larger systems is not only essential to obtain insight but also matters in the design of force fields. For example, the simple point charge water force field[10] deliberately overestimates the dipole moment of a single water because it is widely accepted that its dipole moment is enhanced when in a liquid water environment. In terms of insight, there is growing evidence that proximal water in the vicinity of biological macromolecules behaves differently compared to the bulk solvent. For example, an inelastic incoherent neutron scattering study[11] suggested that one to four layers of water molecules around DNA comprise the interfacial water signal detected.

In their study[12] on water molecules in clusters and ice Ih, Batista et al. employed a variety of partitioning methods to compute molecular multipole moments. The chosen methods all started from the electron density and included the molecular equivalent of the Hirshfeld partitioning technique,[13] two types of Voronoi cells, and the theory of atoms in molecules,[14−16] which we hereafter refer[17] to as quantum chemical topology (QCT). Although these methods all depart from the electron density (for a brief review of alternative nonelectron density methods, see ref 18), they provide quantitatively very different results; the magnitude of the molecular dipole moment in ice Ih ranges between 2.3 and 3.1 D. However, they all agree on the qualitative result of the molecular dipole moment in the ring hexamer being smaller than that in ice Ih. To their analysis the authors added an induction model, a common method for constructing molecular multipoles in a condensed-phase environment, using polarizabilities of the isolated molecule. Unquestionably, the success of this method depends on the (dubious) assumption that the gas-phase polarizability does not significantly differ from that in the cluster or condensed phase.[19]

The current study also focuses on water clusters (but not on ice), on their own and in the presence of the amino acid serine or tyrosine. We limit the analysis to the QCT partitioning method but extend it to more than the dipole moment. The question we ask is not about the convergence of the dipole moment with cluster size but how the charge density is affected by the presence of other molecules and whether we can identify "types" of water molecule with characteristic atomic and molecular properties. This is in line with previous work where we computed, for the first time, atom types[20,21] occurring in the set of all natural amino acids (and smaller derived molecules). This work culminated in recommendations for the design or modification of protein force fields. Here we focus on molecular and atomic properties, in particular, the volume, charge, dipole, and quadrupole moments. Supermolecular

* To whom correspondence should be addressed. E-mail: pla@manchester.ac.uk.

10.1021/jp067922u CCC: $37.00
Published on Web 02/06/2007

electron densities of principal local minima of water clusters (dimer up to nonamer) feature as well as mono- to pentahydrated serine and mono- to pentahydrated tyrosine. Sufficient care was taken to compress the substantial amount of data generated, such that key points can emerge.

2. Background

Quantum topological atoms consist of finite volumes delineated by the gradient vector field of the electron density. Sharp boundaries called interatomic surfaces arise between atoms that share a so-called bond critical point (BCP). The partitioning decision is taken by the topology of the electron density. Since the electron density can be obtained from several sources (e.g., X-ray diffraction, self-consistent field molecular orbital linear combination of atomic orbitals calculations or even quantum monte carlo on a grid), the partitioning is largely model independent. Since atoms do not overlap, and since they exhaust space, they can be simply be added to form a functional group or a molecule in a cluster.

Definitions of the atomic dipole moment are given in eqs 1a−c and those of quadrupole moment components in eqs 2a−e[22]

$$Q_{10}(\Omega) = -\int_{\Omega} d\tau z\rho(\mathbf{r}) \tag{1a}$$

$$Q_{11c}(\Omega) = -\int_{\Omega} d\tau x\rho(\mathbf{r}) \tag{1b}$$

$$Q_{11s}(\Omega) = -\int_{\Omega} d\tau y\rho(\mathbf{r}) \tag{1c}$$

$$Q_{20}(\Omega) = -\int_{\Omega} d\tau \frac{1}{2}(3z^2 - r^2)\rho(\mathbf{r}) \tag{2a}$$

$$Q_{21c}(\Omega) = -\int_{\Omega} d\tau \sqrt{3}xz\rho(\mathbf{r}) \tag{2b}$$

$$Q_{21s}(\Omega) = -\int_{\Omega} d\tau \sqrt{3}yz\rho(\mathbf{r}) \tag{2c}$$

$$Q_{22c} = -\int_{\Omega} d\tau \frac{\sqrt{3}}{2}(x^2 - y^2)\rho(\mathbf{r}) \tag{2d}$$

$$Q_{22s}(\Omega) = -\int_{\Omega} d\tau \sqrt{3}xy\rho(\mathbf{r}) \tag{2e}$$

where $\rho(\mathbf{r})$ is the electron density at a given point $\mathbf{r}$ inside the atomic volume Ω. The tensor expressions in the integrand are expressed in coordinates x, y, and z, with respect to the nucleus of the atom, and $r^2 = x^2 + y^2 + z^2$. Note that the spherical tensor formalism is more compact than the Cartesian, which introduces redundant components. The eqs 2a−e list the five irreducible components constituting the intra-atomic contribution to the total atomic quadrupole moment, and eqs 1a−c similarly the intra-atomic contribution to the atomic dipole moment. The atomic multipole moments can be used in the construction of molecular multipole moments, though not by merely adding the intra-atomic contribution. There is a missing contribution, interatomic in character, which we will now discuss.

We first choose a suitable origin due to the origin dependence of the multipole moments beyond the atomic charge. As the oxygen nucleus is common to all water molecules and lies near the center of mass it is used as a convenient origin throughout this study. The general expression for the molecular multipole moments is expressed relative to this origin, as a summation over "total atomic" contributions (eq 3)

$$Q_{lm}^{\mathrm{tot}} = \sum_{\Omega} Q'_{lm}(\Omega) \tag{3}$$

where $Q_{\mathrm{lm}}^{\mathrm{tot}}$ is component m of the total molecular multipole moment of rank l and $Q'_{lm}(\Omega)$ represents the *total* atomic contribution to the molecular multipole moment. Each total atomic contribution is made up of intra-atomic terms and interatomic terms in eqs 4a−c

$$Q'_{10}(\Omega) = Q_{10}(\Omega) + R_z q(\Omega) \tag{4a}$$

$$Q'_{11c}(\Omega) = Q_{11c}(\Omega) + R_x q(\Omega) \tag{4b}$$

$$Q'_{11s}(\Omega) = Q_{11s}(\Omega) + R_y q(\Omega) \tag{4c}$$

where $\mathbf{R}(R_x, R_y, R_z)$ is the position vector of the atom's nucleus relative to the oxygen and $q(\Omega)$ is the atomic charge. A similar set of expressions (eqs 5a−e) show how the total atomic quadrupole components are constructed

$$Q'_{20}(\Omega) = Q_{20}(\Omega) + 2R_z Q_{10}(\Omega) - R_x Q_{11c}(\Omega) - R_y Q_{11s}(\Omega) + \frac{1}{2}(3R_z^2 - R^2)q(\Omega) \tag{5a}$$

$$Q'_{21c}(\Omega) = Q_{21c}(\Omega) + \sqrt{3}R_z Q_{11c}(\Omega) + \sqrt{3}R_x Q_{10}(\Omega) + \sqrt{3}R_x R_z q(\Omega) \tag{5b}$$

$$Q'_{21s}(\Omega) = Q_{21s}(\Omega) + \sqrt{3}R_z Q_{11s}(\Omega) + \sqrt{3}R_y Q_{10}(\Omega) + \sqrt{3}R_y R_z q(\Omega) \tag{5c}$$

$$Q'_{22c} = Q_{22c}(\Omega) + \sqrt{3}R_x Q_{11c}(\Omega) - \sqrt{3}R_y Q_{11s}(\Omega) + \frac{\sqrt{3}}{2}(R_x^2 - R_y^2)q(\Omega) \tag{5d}$$

$$Q'_{22s} = Q_{22s}(\Omega) + \sqrt{3}R_y Q_{11c}(\Omega) + \sqrt{3}R_x Q_{11s}(\Omega) + \sqrt{3}R_x R_y q(\Omega) \tag{5e}$$

where $Q'_{2m}(\Omega)$ is the total atomic contribution to component m of the (total) molecular quadrupole moment and Q_{2m} (Ω) is component m of the intra-atomic quadrupole moment (eqs 2a−e).

3. Computational Details

The water monomer and pure water clusters shown in Figure 1 were geometry optimized at the B3LYP/aug-cc-pVDZ level to obtain global minima.[23−25] The program GAUSSIAN98[26] was used. For many supermolecular complexes the GDIIS method was crucial to achieve convergence in the geometry optimization. The aug-cc-pVDZ basis set was chosen from recently published results on the accuracy of the electrostatic interaction energy at different levels of theory.[27] Similar optimizations were performed on serine−water clusters (Figure 2) and tyrosine−water clusters (Figure 3), taking the global minimum for pure water as a starting point and substituting the amino acid into the cluster. The alcohol group turned out to preserve the H-bonding network in all cases and to produce a minimum similar to that of the pure water analog. Similar minima have

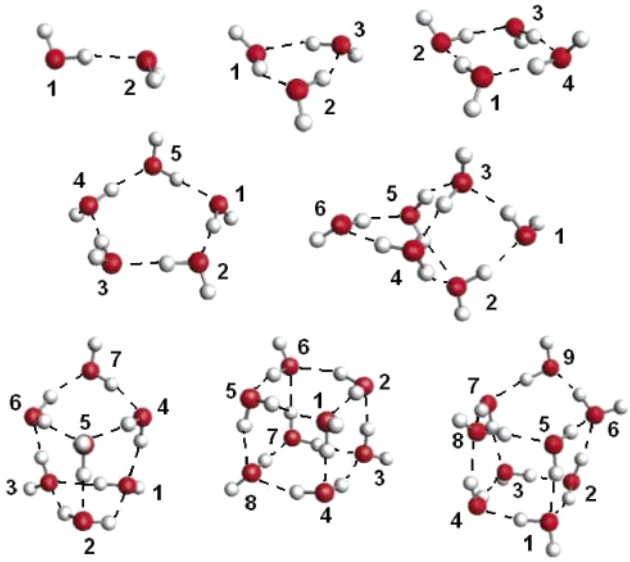

Figure 1. Global minima of water clusters used from dimer through to nonamer. Calculations also include the monomer (not shown).

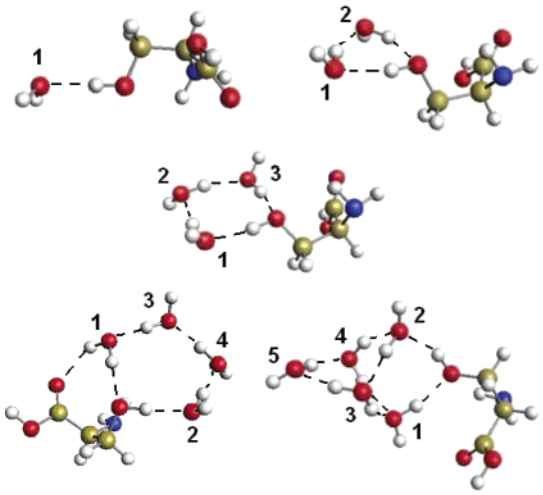

Figure 2. Local minima of serine−water clusters with up to 5 added water molecules. Structures were obtained at the B3LYP/aug-cc-pVDZ level and mimic those of the pure water clusters.

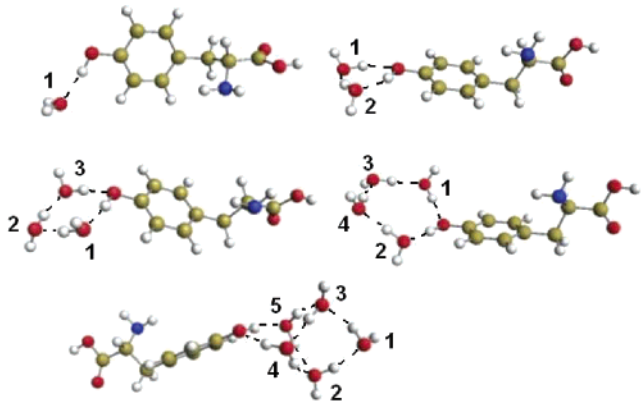

Figure 3. Local minima of tyrosine-water clusters with up to 5 added water molecules. Structures are obtained at the B3LYP/aug-cc-pVDZ level from starting geometries similar to the global minima of pure water clusters.

been observed experimentally and studied theoretically[28] for phenol−water clusters with up to eight water molecules.[29−31] Wave functions were generated by GAUSSIAN98 and passed

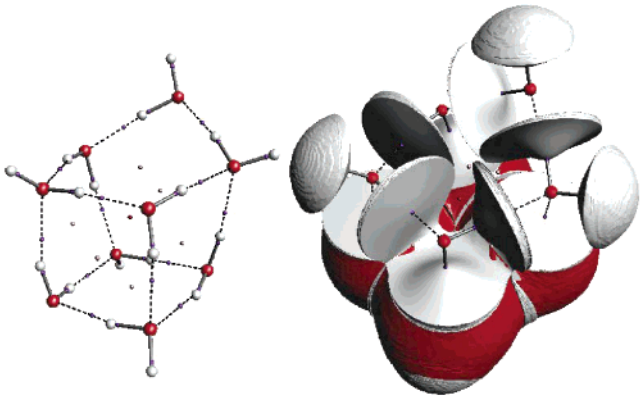

Figure 4. (Left) Atomic interaction lines and critical points in the electron density of the water nonamer. BCPs (purple spheres) lie along atomic interaction lines, ring critical points (pink spheres) appear near the center of each ring in the cluster, and a cage critical point (red sphere) is visible at the center of the cluster. Atomic interaction lines for noncovalent interactions are shown as dotted lines. (Right) Interatomic surfaces and 0.001 au isodensity surfaces of each atom are also shown. The isodensity surfaces of several oxygen atoms in the 5-membered ring have been removed to show the internal structure of the water molecules and the arrangement of the interatomic surfaces relative to the other topological features.

to the program MORPHY98[32] for computation of QCT properties and multipole moments using the compact spherical tensor formalism.[33]

4. Results and Discussion

We find that the B3LYP/aug-cc-pVDZ level of theory yields a molecular dipole moment of 1.857 D for the water molecule, in excellent agreement with the experimental value of 1.855 D.[6,8] The quadrupole moment at this level is 2.846 D·Å, in reasonable agreement with the experimental value of 2.973 D·Å .[34] These results help support the findings of Volkov et al.[27] to give confidence in the quality of our electronic properties.

In Figure 4, we see the results of the topological analysis and partitioning of the charge density of the water nonamer. Atomic interaction lines, visible as ridges between nuclei in the charge density, are shown here as solid sticks where they coincide with traditional bonds and as dotted lines where they represent hydrogen bonds or interactions that are traditionally considered nonbonding. The structure created by the atomic interaction lines demonstrates the cage-like nature of this arrangement, comprising six rings with associated ring critical points and a cage-critical point in the charge density visible at the center. Addition of the interatomic surfaces and outer isodensity surfaces reveals the shape of the component atoms making up the cluster. The flattened appearance of the interior hydrogen atoms clearly differs from the rounded outer atoms.

A similar QCT analysis was performed for all water molecules in each pure water cluster and for those in hydrated serine and tyrosine clusters. Figure 5 shows the volumes, dipole moments, angles of displacement of the dipole moment vector, and quadrupole moments of single water molecules inside all clusters. Note that in this Figure (and Figure 7) only the strongest trends are shown, which is why the label on the *y* axis varies. Sometimes the total number of H-bonds is relevant, sometimes only the number of donated H-bonds, for example.

The volume of each molecule capped by the 0.001 au isodensity surface is heavily dependent on the total number of hydrogen bonds the molecule donates and/or accepts. The effect of hydrogen bonding on the molecular volume is also reflected

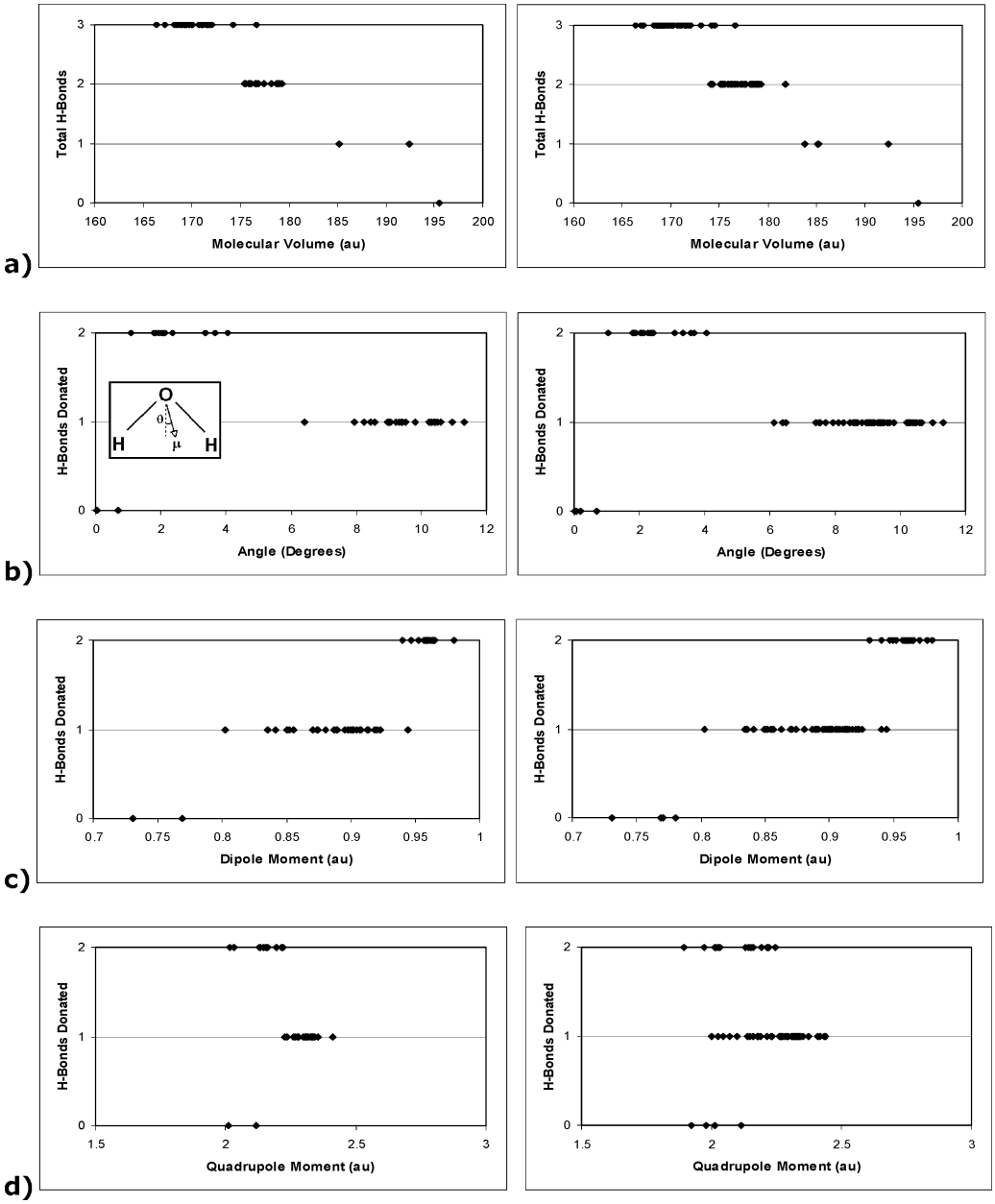

Figure 5. (Left) Molecular properties of a single water molecule in pure water clusters and (right) hydrated serine and tyrosine cluster (right) as a function of the H-bonding environment. Clusters range in size from the water monomer to the nonamer, and serine and tyrosine clusters have up to 5 additional water molecules. (a**)** Molecular volumes are plotted against the sum of H bonds donated and/or accepted. (b**)** The angle of displacement of the dipole moment vector from the symmetrical position is plotted against the number of H-bonds donated by the water molecule. (c**)** The magnitude of the molecular dipole moment is plotted against the number of H bonds donated by the water molecule. (d**)** The magnitude of the molecular quadrupole moment is plotted against the number of H bonds donated by the water molecule.

in the hydrogen atoms of Figure 4 as they are compressed upon contact with the neighboring oxygen, reducing their volume. The more hydrogen bonds a water molecule is involved in, the smaller it becomes. This trend persists when we introduce serine and tyrosine into the water clusters.

Given the absence of any discernible trend in the molecular charge of single water molecules in clusters, this quantity was omitted from Figure 5. Most of the water molecules were almost neutral with a mean absolute charge of 0.005 au, except for the water dimer with the unusually large charge transfer of 0.02 au between monomers.

More interestingly, the molecular dipole moment is systematically affected by the number of hydrogen bonds donated by the water molecule. Previous studies have shown that it increases when moving from the gas-phase monomer to water clusters and the condensed phase.[6,35] We observe that the magnitude of the dipole moment is dependent on the number of hydrogen bonds donated. Furthermore, as there is very little net charge on almost all of the water molecules, this increase must be due to internal rearrangement of the molecular charge density. It is therefore likely that the observed trend toward increased average dipole moment with increased cluster size is a result of each monomer donating, on average, more hydrogen bonds. Water molecules in the dimer donate one H-bond or none, water molecules in the cyclic complexes donate one H-bond, while waters in cage complexes either one or two. Furthermore, the direction of the dipole moment vector varies by over 10° from that of the monomer as the vector is pulled toward a hydrogen-bonded neighbor. As a result, molecules involved in one H-bond have dipole moments significantly more deflected than those

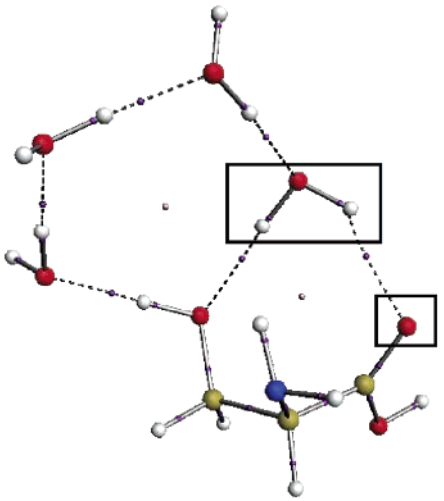

Figure 6. Atomic interaction lines and critical points of the serine••• $(H_2O)_4$ cluster. An extra H bond occurs between the carbonyl oxygen (boxed) of the serine carboxyl group and the hydrogen of an adjacent water molecule (boxed). This leads to a different classification to the corresponding molecule in the pure water pentamer.

bonded to zero or two neighbors (see Figure 5). In other words, the asymmetric environment due to the existence of a H bond on one side and not the other causes the largest deflection in dipole moment. As those molecules that donate two H-bonds rarely show a deflection of less than 2°, we can see that one hydrogen-bonded neighbor generally causes more polarization than the other.

Like a water monomer's dipole moment, the quadrupole moment of a water monomer in pure water clusters is also systematically affected by the number of H-bonds it donates. In contrast to the dipole moment however, the molecular quadrupole moment is largest in molecules that donate a single H bond and has a similar magnitude in the symmetrical "donates 0" and "donates 2" environments. When combining the quadrupole results for pure water clusters with those for clusters incorporating serine and tyrosine, the pattern becomes less clear and there is more overlap between values produced by different H-bonding arrangements. Although not shown in Figure 5, the clear boundaries do still exist in the results for serine−water clusters alone and tyrosine−water clusters alone. Perhaps the presence of the amino acid starts to have an effect when considering the molecular quadrupole moment.

Careful analysis of Figure 5 showed some apparent anomalies in need of further investigation. In particular, the highlighted (by means of a box) water molecule in Figure 6 turned out to have atypical properties for a water molecule expected to donate only one H bond. It was then observed that certain interactions were taking place between this highlighted water and serine's carboxylic acid group. Figure 6 shows this interaction, for which the interacting atoms H and O (boxed) are 2.13 Å apart. This H···O interaction can be classified as a H bond according to the criteria suggested in ref 36. The electron density is 0.017 au at the H···O BCP and the Laplacian of the electron density is 0.052 au. By comparison of bonded and nonbonded radii,[36] the hydrogen atom is penetrated by 0.40 Å and the oxygen by 0.42 Å. When compared to the equivalent hydrogen atom in the pentamer, the H-bonded hydrogen has a smaller volume by 5.6 au, a reduced atomic dipole moment (by 0.03 au), an enhanced positive charge (by 0.03 au), and an increased (i.e., destabilized) atomic energy by 0.015 au. The properties of the labeled water molecule are actually more typical of other water molecules that donate 2 H bonds and accept 1 H bond and differ from the corresponding molecule in the water pentamer and the tyrosine−$(H_2O)_4$ cluster.

The serine−$(H_2O)_5$ cluster shows a similar H···O interaction involving the COOH group, but this time at longer range (2.54 Å). At the corresponding BCP, the electron density is 0.008 au and the Laplacian of the electron density is 0.030 au. The hydrogen atom is penetrated by 0.11 Å and the oxygen by 0.27 Å, which represents a much more unequal penetration than in the case of the previous H bond. The gain in positive charge amounts to 0.014 au and the loss of atomic dipole moment to 0.012 au, while the volume decreases by 1.4 au. However, the atomic energy of the hydrogen is *stabilized* (by 0.022 au). Since the latter observation constitutes a violation of the H-bond criteria,[36] we cannot designate this interaction as a formal H bond. This conclusion is consistent with the properties of the water molecule involved in the interaction (the equivalent of the boxed water molecule in Figure 6). Indeed, its properties lie somewhere between those typical of a molecule donating 2 H bonds and one donating 1 H bond. For the purpose of this study, we therefore classify water molecule 1 of the serine••• $(H_2O)_4$ cluster (see Figure 2) as donating 2 H bonds and molecule 1 of the serine•••$(H_2O)_5$ cluster (again in Figure 2) as donating 1 H bond.

Next we consider the oxygen atoms of the water molecule. Figure 7 contains a similar summary to that for the molecular properties (Figure 5), but now we show the atomic charge. Note that in Figure 5 the absence of molecular charge was justified since all water molecules were almost neutral, without any noticeable trend. Accepting a H bond reduces the volume of the oxygen atom as we might expect. Hence, oxygens accepting 2 H-bonds are the smallest atoms and those that do not accept any H bonds are the largest. What is perhaps unexpected in the serine and tyrosine clusters is the degree of overlap (in Figure 7a) between those oxygen atoms that accept 1 and 2 H bonds. This probably reflects the different internal structures of the clusters with 3-, 4-, and 5-membered rings affecting the shape of the oxygen.

The oxygen atom gradually gains electron density upon formation of more H bonds (Figure 7b). In other words, an oxygen's charge becomes more negative upon increasing the number of H bonds the water molecule (containing this oxygen) is involved in. This is in accord with Hermansson's[37] study of a tetrahedral water cluster, where a migration of electronic charge toward O from both H atoms in the H-accepting molecule was observed. Since the overall molecular charge changes very little upon H-bond formation this gain in negative charge is due to a shift of electron density from the hydrogens toward the oxygen. Hence intramolecular charge transfer dominates the charge rearrangement in all clusters as H-bonds are formed. The water dimer deserves special attention because it shows an unusually large charge transfer (0.02 au) between the constituent water molecules. Even here we see substantial intramolecular transfer toward the oxygen, which gains 0.04 au of negative charge upon H-bond formation.

The reason we see charge transfer in the water dimer and not in the large clusters is that in the latter the transfer between donors and acceptors is approximately balanced.

Figure 7c focuses on the oxygen atomic dipole moment, which decreases with the number of H bonds the molecule donates. This trend is opposite to that observed for the molecular dipole moment. This indicates that the overall increase in molecular dipole moment is largely due to charge transfer

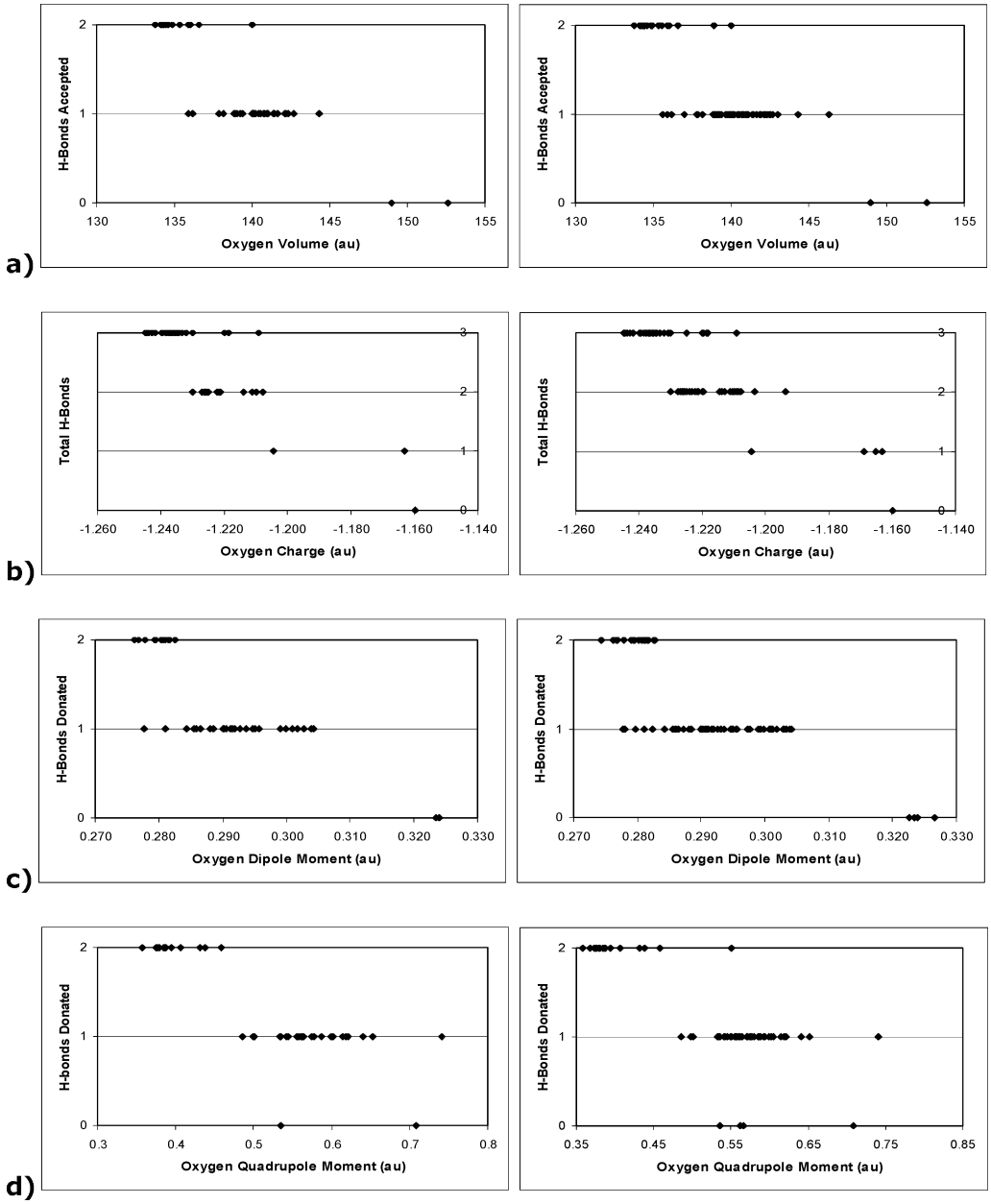

Figure 7. Atomic properties of oxygen atoms in (left) pure water clusters and (right) all clusters, including hydrated serine and tyrosine clusters as a function of H-bonding environment. (a**)** Oxygen atomic volumes are plotted against the number of H bonds accepted by the molecule. (b**)** The atomic charge is plotted against the sum of H-bonds donated and accepted. (c**)** The magnitude of the atomic dipole moment is plotted against the number of H bonds donated by the molecule. (d**)** The magnitude of the atomic quadrupole moment is plotted against the number of H bonds donated by the molecule.

toward the oxygen atom ($q(\Omega)$ term in eqs 4a−c), which is counteracted by the intra-atomic dipole moments (eqs 1a−c).

Figure 7d shows a weak trend in the magnitude of the atomic quadrupole moment, which becomes smaller in molecules that donate two H bonds. This matches the trend seen in the molecular quadrupole moment.

Next we examine the electronic properties of the hydrogen atoms, which are either bonded or nonbonded (Figure 8). All properties are observed to group themselves according to whether atoms are involved in a H bond or not. As expected, we see that H-bonded atoms are smaller and have a wider range of volumes reflecting their different shapes. The H-bonded hydrogens have greater positive charge than the nonbonded hydrogens. The former contribute most to the increased negative charge of the oxygen (in the donor water) upon H-bond formation.

Again the intra-atomic dipole moment is reduced upon H-bond formation, in contradistinction to the molecular dipole moment, backing up the idea that the increase in molecular dipole moment is caused by intramolecular charge transfer toward the oxygen. The magnitude of the intra-atomic quadrupole moment generally increases upon involvement in a H bond, as was the case for the molecular quadrupole moment. Finally, we find that the atomic kinetic energy decreases, probably due to the decrease in the electron population of the atom.

We are now in a position to identify water molecule types with electronic properties that fall within a characteristic range based on features of their H-bonding environment. Figure 9 illustrates the H-bonding environments encountered by the water molecules in different clusters. The colors represent different

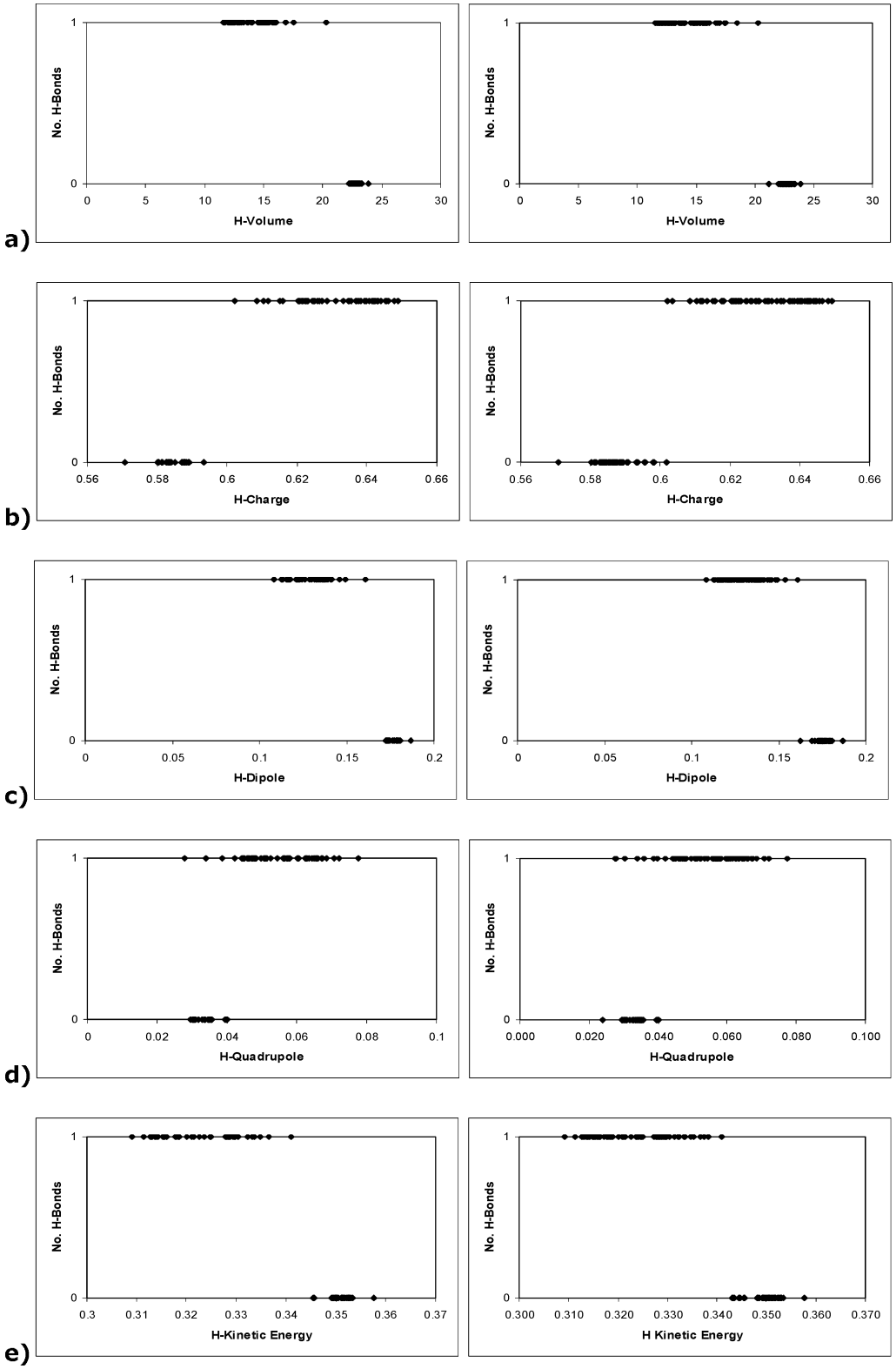

Figure 8. Atomic properties of hydrogen atoms in (left) pure water clusters and (right) all clusters, including hydrated serine and tyrosine clusters. Charts show (a**)** hydrogen atomic volumes, (b**)** hydrogen atomic charges, (c**)** the magnitude of the atomic dipole moment, (d**)** the magnitude of the atomic quadrupole moment, and (e**)** the total atomic kinetic energy comparing those atoms that are involved in a H bond with those that are unbound.

environments that will determine the electronic properties. Table 1 summarizes the classifications that can be made.

Finally, Figure 10 shows the water nonamer with the only two different H-bonding environments that determine the molecular dipole moment for this cluster; molecules that donate two H bonds are distinguished from those that donate only one. Hopefully the ability to predict the dipole moment based solely on the H-bonding environment will ultimately enable force fields to quickly determine molecule or atom types. Such force fields could then account for polarization by mimicking intramolecular

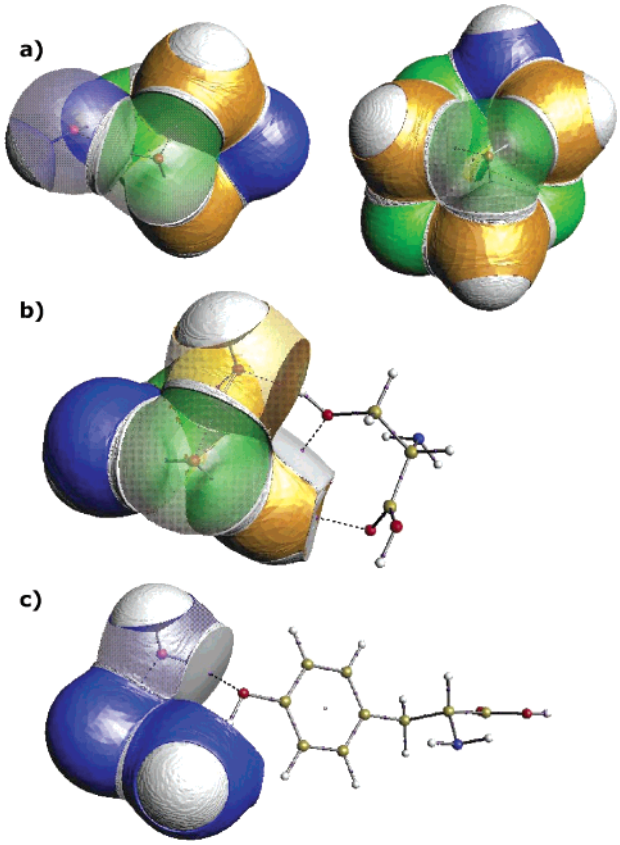

Figure 9. Colored isodensity surfaces of water molecules representing different H-bonding environments. Selected surfaces are made transparent to reveal topological features beneath. Blue water molecules donate 1 H bond to other molecules and accept 1, orange water molecules donate 1 H bond and accept 2, and green molecules donate 2 and accept 1. (a) Water molecules in the water hexamer (left) and nonamer (right). Oxygen atoms have been colored according to the H-bonding environment of the water molecule. (b) Water molecules in serine$\cdots(H_2O)_5$ cluster. (c) Water molecules in the tyrosine$\cdots(H_2O)_3$ cluster, all colored blue as they share an identical H-bonding environment.

Figure 10. Isodensity surface ($\rho = 0.001$ au) of water molecules in the nonamer. Selected transparent surfaces reveal topological features beneath. The two environments present in the nonamer that affect molecular dipole moment are shown using different colored oxygen atoms. Molecules donating 1 H bond are marked in blue, and those donating 2 H bonds are marked in green.

charge transfer. A similar approach could be used for the molecular quadrupole moment, although more work must first be carried out into which components are affected and by how much.

TABLE 1: Effect of the H-Bonding Environment on Atomic and Molecular Properties Measured by the Properties' Range and Mean Value in Clusters of Pure Water and Hydrated Serine and Tyrosine Clusters (All Values Are Given in Atomic Units Except the Dipole Angle Which Is in Degrees)

property	category	min	max	mean
molecular volume	total H bonds = 0	195.5	195.5	195.5
	total H bonds = 1	183.8	192.4	186.7
	total H bonds = 2	174.1	181.9	177.2
	total H bonds = 3	166.4	176.7	170.1
molecular dipole moment	donates 0 H bonds	0.730	0.781	0.763
	donates 1 H bond	0.803	0.944	0.889
	donates 2 H bonds	0.931	0.980	0.958
molecular dipole angle[a]	donates 0 H bonds	0.0	0.7	0.2
	donates 1 H bond	6.1	11.3	9.2
	donates 2 H bonds	1.1	4.1	2.5
molecular quadrupole moment (pure waterclusters only)	donates 0 H bonds	2.012	2.116	2.064
	donates 1 H bond	2.229	2.411	2.312
	donates 2 H bonds	2.016	2.221	2.149
oxygen volume	accepts 0 H Bonds	149.0	152.6	150.8
	accepts 1 H Bond	135.6	146.3	140.3
	accepts 2 H Bonds	133.8	140.0	135.4
oxygen charge	total H bonds = 0	−1.160	−1.160	−1.160
	total H bonds = 1	−1.204	−1.163	−1.175
	total H bonds = 2	−1.230	−1.194	−1.219
	total H bonds = 3	−1.245	−1.209	−1.234
oxygen dipole moment	donates 0 H bonds	0.323	0.327	0.324
	donates 1 H bond	0.278	0.304	0.292
	donates 2 H bonds	0.274	0.283	0.280
oxygen quadrupole moment	donates 0 H bonds	0.535	0.709	0.593
	donates 1 H bond	0.485	0.741	0.573
	donates 2 H bonds	0.358	0.551	0.399
hydrogen volume	not H bonded	21.2	23.9	22.6
	H bonded	11.5	20.3	14.1
hydrogen charge	not H bonded	0.571	0.602	0.587
	H bonded	0.602	0.649	0.630
hydrogen dipole moment	not H bonded	0.162	0.187	0.175
	H bonded	0.108	0.161	0.128
hydrogen quadrupole moment	not H bonded	0.024	0.040	0.033
	H bonded	0.028	0.078	0.054
hydrogen kinetic energy	not H bonded	0.343	0.358	0.350
	H bonded	0.309	0.341	0.323

[a] The molecular dipole angle is the deviation of the dipole vector from the symmetrical case where it lies half way between the hydrogen atoms (as in the water monomer).

5. Conclusion

The effect of the H-bonding environment on the charge density of water molecules in clusters and hydrated amino acid systems has been investigated. Water molecules remain virtually neutral when present in the clusters studied. The polarization due to H-bond formation takes place by electronic charge transfer from the hydrogen atoms of the water molecule to the oxygen. The atomic dipole moments (i.e., intra-atomic contributions only) are actually reduced in this process. However, the charge-transfer term is large enough to produce a net increase in molecular dipole moment. The direction of the dipole moment

is changed as it is pulled toward the bond being formed. Overall, intramolecular charge transfer dominates the charge rearrangement in all clusters as H bonds are formed. Similar trends are observed for the molecular quadrupole moment, although the largest values occur in molecules that donate one H-bond, and smaller values appear in the symmetrical environments with zero or two H bonds donated.

We observe that atomic and molecular properties of the charge density lie within characteristic ranges of values depending on their H-bonding environment. It is therefore possible to categorize types of water molecule with specific electronic characteristics based on H-bonds formed. Conversely, given the local environment of a water molecule in a cluster we are able to estimate values for its electronic properties.

Acknowledgment. We thank the EPSRC and GlaxoSmith-Kline for financial support.

References and Notes

(1) Barnes, P.; Finney, J. L.; Nicholas, J. D.; Quinn, J. E. *Nature* **1979**, *282*, 459.

(2) Goodfellow, J. M. *Proc. Natl. Acad. Sci. U.S.A.* **1982**, *79*, 4977.

(3) Simons, J. P.; Jockusch, R. A.; Carcabal, P.; Huenig, I.; Kroemer, R. T.; Macleod, N. A.; Snoek, L. C. *Intern. Rev. Phys. Chem.* **2005**, *24*, 489.

(4) Abo-Riziq, A. G.; Crews, B.; Bushnell, J. E.; Callahan, M. P.; DeVries, M. S. *Mol. Phys.* **2005**, *103*, 1491.

(5) Hobza, P.; Zahradnik, R.; Mueller-Dethlefs, K. *Collect. Czech. Chem. Commun.* **2006**, *71*, 443.

(6) Gregory, J. K.; Clary, D. C.; Liu, K.; Brown, M. G.; Saykally, R. J. *Science* **1997**, *275*, 814.

(7) Batista, E. R.; Xantheas, S. S.; Jonsson, H. *J. Chem. Phys.* **1999**, *111*, 6011.

(8) Clough, S. A.; Beers, Y.; Klein, G. P.; Rothman, L. S. *J. Chem. Phys.* **1973**, *59*, 2254.

(9) Xantheas, S. S.; Dunning, T. H. *J. Chem. Phys.* **1993**, *99*, 8774.

(10) Berendsen, H.; Postma, J.; Van Gunsteren, W.; Hermans, J. *Intermolecular Forces*; 1981.

(11) Ruffle, S.; Michalarias, I.; Li, J.; Ford, R. *J. Am. Chem. Soc.* **2001**, *124*, 565.

(12) Batista, E.; Xantheas, S.; Jonsson, H. *J. Chem. Phys.* **1999**, *111*, 6011.

(13) Hirshfield, F. *Theor. Chim. Acta* **1977**, *44*, 129.

(14) Bader, R. F. W. *Atom in Molecules. A Quantum Theory*; Oxford University Press, 1990.

(15) Bader, R. F. W.; Tal, Y.; Anderson, S. G.; Nguyen-Dang, T. T. *Isr. J. Chem.* **1980**, *19*, 8.

(16) Popelier, P. L. A. *Atoms in Molecules. An Introduction.*; Pearson: London, Great Britain, 2000.

(17) Popelier, P. L. A.; Aicken, F. M. *Chem. Phys. Chem.* **2003**, *4*, 824.

(18) Popelier, P. L. A.; Devereux, M.; Rafat, M. *Acta Cryst.* **2004**, *A60*, 427.

(19) Yang, M.; Senet, P.; Van Alsenoy, C. *Int. J. Quant. Chem.* **2003**, *101*, 535.

(20) Popelier, P. L. A.; Aicken, F. M. *Chem.−Eur. J.* **2003**, *9*, 1207.

(21) Popelier, P. L. A.; Aicken, F. M. *J. Am. Chem. Soc.* **2003**, *125*, 1284.

(22) Buckingham, A. D. *J. Chem. Phys.* **1959**, *30*, 1580.

(23) Wales, D.; Hodges, M. *Chem. Phys. Lett.* **1998**, *286*, 65.

(24) Goldman, N.; Saykally, R. *J. Chem. Phys.* **2004**, *120*, 4777.

(25) Wales, D. J.; Doye, J. P. K.; Dullweber, A.; Hodges, M. P.; Naumkin, F. Y.; Calvo, F.; Hernández-Rojas, J.; Middleton, T. F. *The Cambridge Cluster Database*.

(26) Frisch, M. J.; G. W. T., Schlegel, H. B.; Scuseria, G. E.; Robb, M. A.; Cheeseman, J. R.; Zakrzewski, V. G.; Montgomery, J. A. Jr.; Stratmann, R. E.; Burant, J. C.; Dapprich, S.; Millam, J. M.; Daniels, A. D.; Kudin, K. N.; Strain, M. C.; Farkas, O.; Tomasi, J.; Barone, V.; Cossi, M.; Cammi, R.; Mennucci, B.; Pomelli, C.; Adamo, C.; Clifford, S.; Ochterski, J.; Petersson, G. A.; Ayala, P. Y.; Cui, Q.; Morokuma, K.; Malick, D. K.; Rabuck, A. D.; Raghavachari, K.; Foresman, J. B.; Cioslowski, J.; Ortiz, J. V.; Baboul, A. G.; Stefanov, B. B.; Liu, G.; Liashenko, A.; Piskorz, P.; Komaromi, I.; Gomperts, R.; Martin, R. L.; Fox, D. J.; Keith, T.; Al-Laham, M. A.; Peng, C. Y.; Nanayakkara, A.; Gonzalez, C.; Challacombe, M.; Gill, P. M. W.; Johnson, B.; Chen, W.; Wong, M. W.; Andres, J. L.; Gonzalez, C.; Head-Gordon, M.; Replogle, E. S.; Pople, J. A. *Gaussian 98*; Gaussian Inc.: Pittsburgh, 1998.

(27) Volkov, A.; King, H.; Coppens, P. *J. Chem. Theor. Comput.* **2006**, *2*, 81.

(28) Tsui, H. H. Y.; van Mourik, T. *Chem. Phys. Lett.* **2001**, *350*, 565.

(29) Watanabe, H.; Iwata, S. *J. Chem. Phys.* **1996**, *105*, 420.

(30) Watanabe, T.; Ebata, T.; Tanabe, S.; Mikami, N. *J. Chem. Phys.* **1996**, *105*, 408.

(31) Janzen, C.; Spangenberg, D.; Roth, W.; Kleinermanns, K. *J. Chem. Phys.* **1999**, *110*, 9898.

(32) Popelier, P. L. A. *Morphy98*; UMIST, Manchester, England: Manchester, 1998.

(33) Stone, A. J. *The Theory of Intermolecular Forces*; Oxford, Clarendon Press, 1996.

(34) Verhoeven, J.; Dymanus, A. *J. Chem. Phys.* **1970**, *52*, 3222.

(35) Silvestrelli, P. L.; Parrinello, M. *Phys. Rev. Lett.* **1999**, *82*, 5415.

(36) Koch, U.; Popelier, P. L. A. *J. Phys. Chem.* **1995**, *99*, 9747.

(37) Hermansson, K. *J. Chem. Phys.* **1988**, *89*, 2149.